CHEMISTRY OF MATERIALS

Article

pubs.acs.org/cm

Nanostructured Two-Component Liquid-Crystalline Electrolytes for High-Temperature Dye-Sensitized Solar Cells

Daniel Högberg,[†,‡] Bartolome Soberats,[†] Satoshi Uchida,[§] Masafumi Yoshio,[†] Lars Kloo,[‡] Hiroshi Segawa,[§] and Takashi Kato*[,†]

[†]Department of Chemistry and Biotechnology, School of Engineering, The University of Tokyo, Hongo, Bunkyo-ku, Tokyo 113-8656, Japan

[‡]Applied Physical Chemistry, KTH Royal Institute of Technology, SE 100 44 Stockholm, Sweden

[§]Research Center for Advanced Science and Technology, The University of Tokyo, Komaba, Meguro-ku, Tokyo 153-8904, Japan

Supporting Information

ABSTRACT: Nanostructured liquid-crystalline (LC) ion transporters have been developed and applied as new electrolytes for dye-sensitized solar cells (DSSCs). The new electrolytes are two-component liquid crystals consisting of a carbonate-based mesogen and an ionic liquid that self-assemble into two-dimensional (2D) nanosegregated structures forming well-defined ionic pathways suitable for the I^-/I_3^- redox couple transportation. These electrolytes are nonvolatile and they show LC phases over wide temperature ranges. The DSSCs containing these electrolytes exhibit exceptional open-circuit voltages (V_{oc}) and improved power conversion efficiencies with increasing temperature. Remarkably, these solar cells operate at temperatures up to 120 °C, which is, to the best of our knowledge, the highest working temperature reported for a DSSC. The nature of the LC electrolyte and the interactions at the TiO_2 electrode/electrolyte interface lead to a partial suppression of electron recombination reactions, which is key in the exceptional features of these LC-DSSCs. Thus, this type of solar cells are of interest, because they can produce electricity efficiently from light at elevated temperatures.

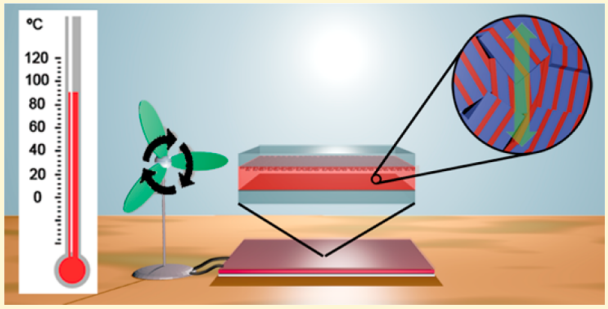

INTRODUCTION

Self-assembled organic molecules forming well-defined pathways for the transport of molecules or ions have been attracting increased attention as functional materials.[1−10] One-dimensional (1D),[11,12] two-dimensional (2D),[13] and three-dimensional (3D)[14−16] nanostructured materials have been developed on the basis of self-assembly of ionic liquid crystals.[17−20] In particular, imidazolium- and ammonium-based compounds have been shown to be versatile to obtain self-assembled ion conductors with potential application in energy devices.[11−14,21] We previously proposed 2D anisotropic ion conductors based on liquid-crystalline (LC) layered nanostructures. They showed new features to be used as electrolyte materials.[13] Yanagida and Watanabe used this concept for the preparation of a dye-sensitized solar cell (DSSC) using a smectic (Sm) imidazolium liquid crystal containing the I^-/I_3^- redox pair as an electrolyte.[22,23] Most recently, by using similar imidazolium-based liquid crystals, Guldi and co-workers found that these LC-DSSCs show improved power conversion efficiencies (PCEs) upon heating.[24] This type of DSSCs could be important for the development of photovoltaic devices capable of functioning efficiently at high temperature. However, their operation mechanism is not well-known and they still show relatively low open-circuit voltage (V_{oc}) and PCEs. Understanding these systems is challenging and important in order to improve the electrolyte materials and the DSSCs. We think that a more flexible material design of the LC electrolytes may lead to an improvement in efficiency of the LC-DSSCs and extend their working temperature ranges. Previously, we reported on thermotropic ionic liquid crystals formed from the dynamic supramolecular assemblies raising between ionic liquids and amphiphilic mesogenic molecules.[13,25−27] These two-component materials exhibit higher ionic conductivities than the analogous single-component ionic liquid crystals.[25] If we use such a strategy, highly tunable mixtures can be obtained, whose physical properties and components ratio can be modified and optimized for application as electrolytes in DSSCs. Herein we report on the development of DSSCs based on new two-component LC electrolytes (Figure 1) with wide temperature ranges of LC phases. These LC electrolyte-based solar cell devices exhibit improved PCEs and exceptional V_{oc} values. Moreover, they show a remarkable increase in PCEs upon heating from 30 °C to 90 °C and can convert light to electricity at temperatures up to 120 °C. These results highlight this type

Received: August 22, 2014
Revised: October 20, 2014
Published: October 21, 2014

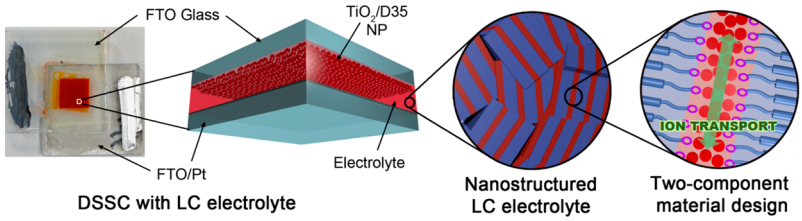

Figure 1. Schematic illustration of the liquid-crystalline (LC) dye-sensitized solar cell (DSSC) and the proposed organization of the two-component nanostructured electrolyte. Blue areas represent the lipophilic parts and red areas represent the hydrophilic parts. [FTO = fluoride-doped tin oxide, NP = nanoparticles.]

of LC-based materials as promising electrolytes for use in DSSCs at elevated temperatures.

DSSCs have attracted great attention, because of their relatively good performance and potentially inexpensive manufacturing cost.[28] They generally consist of a dye-coated (sensitized) semiconductor oxide, such as TiO_2, as the working electrode, a platinized transparent conducting oxide substrate as the counter electrode, and an electrolyte containing a suitable redox couple.[29] Initially, organic solvents containing the I^-/I_3^- redox couple were used as electrolytes.[28,29] However, organic solvent-based solar cells are sensitive to leakage and solvent evaporation; therefore, their use at high temperature is not suitable.[30] In order to overcome these issues, nonvolatile electrolytes, such as composites,[31,32] polymers,[33,34] ionic liquids (ILs),[35−37] and inorganic hole-conducting materials,[38] have been studied as alternatives. These new materials may solve the problems of leakage and evaporation, but they all suffer from a decrease in PCE at elevated temperatures.[39−41] Not much information about the temperature dependence of electrolytes has been reported in the literature, except for IL-based electrolytes.[42−46] Generally, solar cells tend to show a decrease in performance above 50 °C.[41] Thus, it is important to develop devices capable of efficiently functioning at high temperature, which may widen their area of application.

In the present study, we designed a new two-component LC electrolyte for DSSCs, consisting of the carbonate-based mesogenic molecule **1** and IL **2** (Figure 2a). This material generates the I_3^- anions in the presence of I_2 (Figure 2). Through this approach, it was expected to obtain thermally stable and nonvolatile LC electrolytes capable of transporting the essential I^-/I_3^- redox couple (Figure 2b) in a wide temperature range. The new feature of this material is the two-component system. The mesogenic moiety of **1** may contribute to stabilization of the LC phases while the carbonate groups interact with the ionic species and drive the formation of well-defined ionic pathways (Figure 2b). IL **2** was chosen as iodide source and provides the I^-/I_3^- redox pair after the addition of iodine. This electrolyte design was expected to improve the LC-DSSCs performances and widen their working temperature ranges.

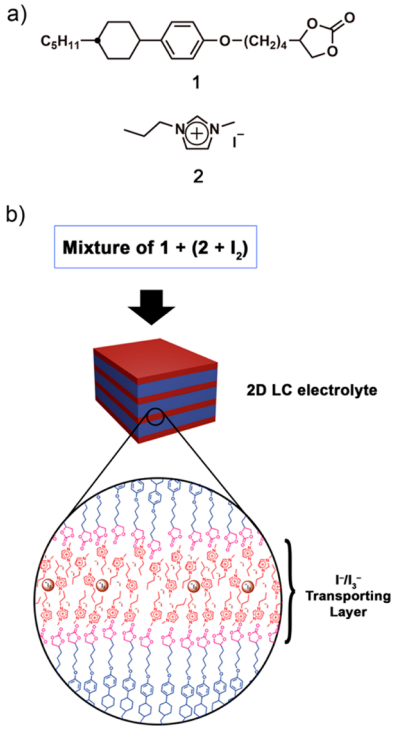

Figure 2. (a) Chemical structure of compounds **1** and **2**. (b) Schematic representation of the two-component LC electrolytes based on the mixtures of **1**, **2**, and I_2.

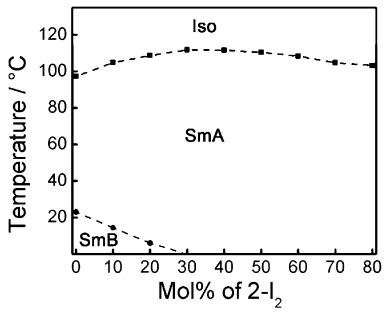

Figure 3. Phase diagram of mixtures **1** and **2**-I_2, as a function of temperature and mole percentage of **2**-I_2. Phase transition temperatures were determined from the transition peaks of the differential scanning calorimetries. Transition temperatures were taken during the second heating process (10 °C min^{-1}). [Iso = isotropic; SmA = smectic A; SmB = smectic B.]

RESULTS AND DISCUSSION

Preparation of Two-Component LC Electrolytes. The new electrolytes (**1**/**2**-I_2) were prepared by mixing **1** and the mixture **2**-I_2, composed of **2** with 20 mol % of I_2, in different ratios. The LC behavior of the mixtures was determined by polarizing optical microscopy (POM) observations, X-ray diffraction (XRD), and differential scanning calorimetry (DSC). Figure 3 shows the phase diagram of the mixtures as a function of the mole percentage of **2**-I_2. All the mixtures exhibit smectic A (SmA) LC phases in wide temperature ranges. The single component of **1** and the mixtures containing 10, 20, and 30 mol % of **2**-I_2 also show smectic B phases at low temperatures. After addition of more than 80 mol % of **2**-I_2 to **1**, no homogeneous LC phases were observed due to phase

dx.doi.org/10.1021/cm503090z | Chem. Mater. 2014, 26, 6496−6502

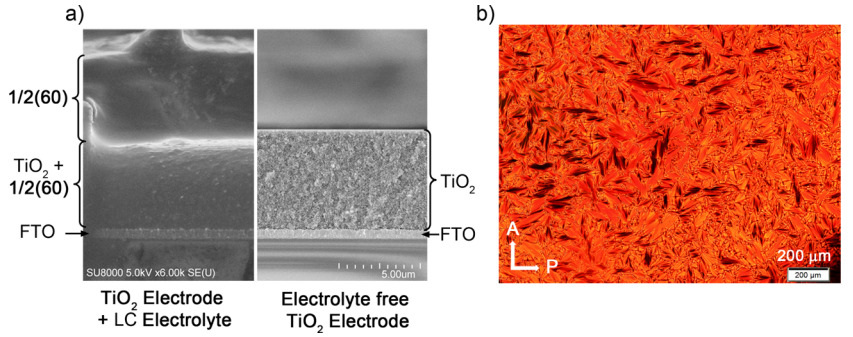

Figure 4. (a) Scanning electron microscopy (SEM) micrograph of the cross-section of TiO_2 electrodes containing **1/2-I$_2$(60)** (left) and electrolyte-free TiO_2 electrodes (right). (b) Polarizing optical microscopy (POM) image of a DSSC that contains **1/2-I$_2$(60)** at 30 °C.

separation. The XRD patterns at 30 °C of the **1/2-I$_2$** mixtures showed four peaks with a reciprocal *d*-spacing ratio of 1:2:3:4. These peaks correspond to the (001), (002), (003), and (004) reflections of SmA phases (see the Supporting Information). The interlayer distances of the SmA phases were estimated from the XRD patterns (see the Supporting Information). In the **1/2-I$_2$** mixtures, the distance between layers increases with increasing amounts of **2-I$_2$** (again, see the Supporting Information). This observation confirms the formation of homogeneous mixtures and indicates that the IL is incorporated in the layered nanostructure (Figure 2b).

Structure and Photovoltaic Properties of LC-DSSCs. Mixtures of **1** with 50 mol % **2-I$_2$** [**1/2-I$_2$(50)**], 60 mol % **2-I$_2$** [**1/2-I$_2$(60)**] and 70 mol % **2-I$_2$** [**1/2-I$_2$(70)**] were selected for their use as electrolytes in DSSCs. The electrolyte mixtures were sandwiched between a dye-sensitized TiO_2 electrode and a platinized fluoride-doped tin oxide (FTO) counter electrode. To obtain appropriate penetration of the electrolyte into the porous TiO_2 structure, the cells were heated over the isotropization temperature before the current–voltage (*I*–*V*) measurements. Figure 4a shows the scanning electron microscopy (SEM) images of a TiO_2 electrode cross section before and after addition of the LC electrolyte. The porous texture of the TiO_2 film cannot be observed after addition of the mixture. This observation confirms that the electrolyte had penetrated well into the porous TiO_2 electrode. In addition, the LC organization inside the assembled cells was observed with a polarized optical microscopy (POM) system. The polarizing optical micrograph of a DSSC containing **1/2-I$_2$(60)** (Figure 4b) shows randomly oriented microdomains which are invariant between room temperature (rt) and 90 °C. The *I*–*V* characteristics of the assembled LC-DSSCs were measured at different temperatures under standard air mass 1.5 global sunlight (AM 1.5G) (see Figure 5 and the Supporting Information). Figure 5 shows the *I*–*V* curves of a **1/2-I$_2$(60)**-DSSC at 30 and 90 °C. The shape of the curves significantly changes, probably due to a decrease in the resistance of the cell. The photovoltaic parameters at 30 and 90 °C of the **1/2-I$_2$(50)**, **1/2-I$_2$(60)**, **1/2-I$_2$(70)** LC-DSSCs and the **2-I$_2$** IL-DSSCs, which was used as reference, are shown in Table 1. The LC-based DSSCs show higher V_{oc} than the **2-I$_2$**-based cells. The **1/2-I$_2$(60)**-based device exhibits a V_{oc} value of up to 0.84 V at 30 °C, which is high for a system that contains the D35 sensitizer[47,48] and an I^-/I_3^--based electrolyte. Moreover, the values of short-circuit current densities (J_{sc}), fill factor (FF), and PCE of the LC-DSSCs are much higher at 90 °C than at 30 °C. This tendency is not observed for the cells containing only **2-I$_2$**, which suffers a large drop in PCE at 90

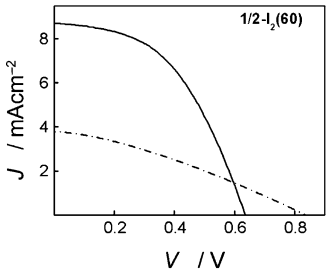

Figure 5. Current–voltage (*I*–*V*) curves for **1/2-I$_2$(60)**-based DSSC at 30 (dash-dotted line) and 90 °C (solid line) under air mass 1.5 global (AM 1.5 G) illumination (1000 W m^{-2}).

°C. The best efficiencies among the LC-based devices are observed for the cells containing **1/2-I$_2$(60)**, which exhibits PCE values of up to 1.8% at 30 °C and 2.7% at 90 °C. To the best of our knowledge, the **1/2-I$_2$(60)**-based cell exhibits the highest V_{oc} reported for DSSCs that contain LC electrolytes.

Temperature Behavior of LC-DSSCs. The major advantages of LC-DSSCs lie in the nonvolatile and thermally stable properties of the LC electrolytes. Thus, the use of these electrolyte materials may allow the development of solar cells that can operate efficiently at elevated temperatures, which is one of the most challenging issues in solar cell technology.[41] In order to obtain more information about the thermal behavior of the **1/2-I$_2$** and the **2-I$_2$**-based solar cells, their photovoltaic parameters were monitored during heating and cooling processes between 30 and 90 °C (see the Supporting Information). The PCE, FF, J_{sc}, and V_{oc} values of a **1/2-I$_2$(60)**-based DSSC and a **2-I$_2$**-based DSSC are plotted as a function of temperature in Figure 6. Interestingly, the PCE gradually increase from 30 °C to 90 °C for the cell containing **1/2-I$_2$(60)**, while the **2-I$_2$**-containing cell exhibits a gradual decrease on heating (Figure 6). Moreover, the **1/2-I$_2$(60)**-based DSSC show a remarkable increase in FF and J_{sc} with increasing temperature and a slight decrease in V_{oc}. Considering that the PCE is proportional to FF, J_{sc} and V_{oc},[29] it seems that the increase in J_{sc} and FF compensates the loss in V_{oc}. Such behavior is not observed for the **2-I$_2$**-based DSSC, where the J_{sc} and FF decrease as the temperature increases.

Table 2 shows the photovoltaic parameters of a **1/2-I$_2$(60)**-based DSSC at 100, 110, and 120 °C. All photovoltaic parameters gradually decrease at temperatures over 90 °C. No significant change was observed in this tendency after isotropization of the electrolyte (108 °C). It should be highlighted that the **1/2-I$_2$(60)**-based DSSC can operate until

dx.doi.org/10.1021/cm503090z | *Chem. Mater.* 2014, 26, 6496–6502

Table 1. Photovoltaic Parameters for DSSCs Containing Different Electrolyte Mixtures at 30 and 90 °C[a]

mixture	temperature, T(°C)	open-circuit voltage, V_{oc} (V)	short-circuit current density, J_{sc} (mA cm^{-2})	fill factor, FF (%)	power conversion efficiency, PCE[b] (%)
1/2-I$_2$(50) (50 mol % **2-I$_2$**)	30	0.70 ± 0.05	2.0 ± 1.1	41 ± 7	0.6 ± 0.3
	90	0.58 ± 0.03	7.6 ± 0.5	48 ± 3	2.1 ± 0.2
1/2-I$_2$(60) (60 mol % **2-I$_2$**)	30	0.78 ± 0.06	4.3 ± 0.9	36 ± 6	1.3 ± 0.5
	90	0.58 ± 0.07	8.2 ± 0.5	52 ± 6	2.5 ± 0.2
1/2-I$_2$(70) (70 mol % **2-I$_2$**)	30	0.71 ± 0.08	3.8 ± 1.1	33 ± 1	0.9 ± 0.2
	90	0.52 ± 0.08	7.9 ± 0.6	58 ± 5	2.4 ± 0.2
2-I$_2$	30	0.58 ± 0.03	8.5 ± 0.4	62 ± 1	2.9 ± 0.4
	90	0.39 ± 0.02	7.1 ± 0.2	49 ± 2	1.5 ± 0.1

[a]Average values and standard deviations of the photovoltaic parameters were calculated from three devices for each electrolyte. [b]Measurements were recorded under AM 1.5 G illumination (1000 W m^{-2}).

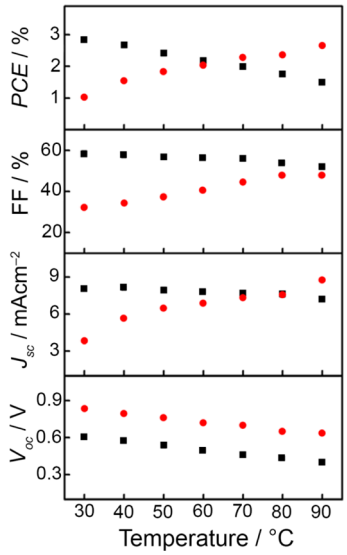

Figure 6. Power conversion efficiency (PCE), fill factor (FF), short-circuit current density (J_{sc}), and open-circuit voltage (V_{oc}) of a DSSC containing **1/2-I$_2$(60)** (red circles) and a DSSC containing **2-I$_2$** (black squares) as a function of temperature. All measurements were conducted under AM 1.5 G illumination (1000 W m^{-2}) during a heating process.

Table 2. Photovoltaic Parameters for a DSSC Containing 1/2-I$_2$(60) at Elevated Temperatures[a]

temperature, T (°C)	open-circuit voltage, V_{oc} (V)	short-circuit current density, J_{sc}[f] (mA cm^{-2})	fill factor, FF[g] (%)	power conversion efficiency, PCE[h] (%)
100[b]	0.49	7.84	58	2.2
110[b,c]	0.44	7.76	57	2.0
120[b,c]	0.41	7.32	56	1.7

[a]The photovoltaic parameters were recorded under AM 1.5 G illumination (1000 W m^{-2}). [b]The cells were assembled using a Bynel (50 μm) spacer. [c]Temperature over the isotropic point of the LC electrolyte (108 °C). [f]Short-circuit current density. [g]Fill factor. [h]Power conversion efficiency.

120 °C, which, to the best of our knowledge, is the highest working temperature reported for a DSSC.

Effects of LC Electrolytes on LC-DSSCs. Guldi and co-workers previously observed an increase in PCE by heating their DSSCs that contained LC dialkylimidazolium electrolytes.[24] They proposed that this phenomenon is related to changes in ion transport, viscosity, and electrode coverage of the electrolytes with the change in temperature, as well as the characteristics of the ordered LC phases.[24] This is a general explanation, but it does not describe the exact role of the LC electrolytes. In the present work, we have performed a comparative study, comprising LC- and IL-based DSSCs, wherein we attempted to obtain information about the role of the LC nanostructured electrolytes. For this purpose, we studied the thermal behavior of FF, J_{sc}, and V_{oc} of the **1/2-I$_2$**- and **2-I$_2$**-based cells (see Figure 6 and the Supporting Information). In addition, we measured the I_3^- diffusion coefficient (D) of the electrolytes, the total electrical resistance (R_s),[49] and electron lifetime (τ) of the LC- and IL-based DSSCs, as a function of temperature (Figure 7 and the Supporting Information). Interestingly, we found that the key to the LC-DSSCs thermal behavior is related to a partial suppression of the electron recombination reaction at the TiO_2-

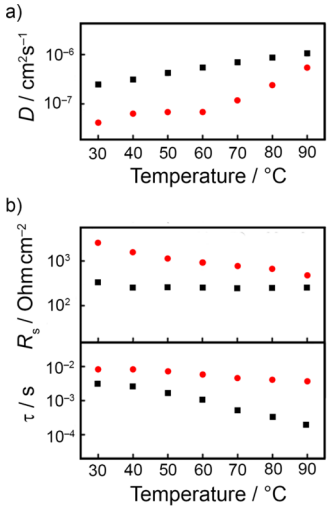

Figure 7. (a) I_3^- diffusion coefficients (D) of the **1/2-I$_2$(60)** (red circles) and **2-I$_2$** (black squares) electrolytes, as a function of temperature (top). (b) Total electrical resistance (R_s) (top) and electron lifetime (τ) (bottom) for the **1/2-I$_2$(60)**-based DSSCs (red circles) and **2-I$_2$**-based DSSCs (black squares), as a function of temperature. The I–V curves and electrochemical impedance experiments used to obtain R_s and τ, respectively, were recorded under AM 1.5 G illumination (1000 W m^{-2}).

dx.doi.org/10.1021/cm503090z | Chem. Mater. 2014, 26, 6496–6502

electrode/electrolyte interface. We believe that this phenomenon arises from the interactions between the electrode surface and the nanostructured LC electrolyte.

Initially, we focused our study on the mass transport properties of the electrolytes. It is well-known that ILs and IL crystals usually exhibit increases in ionic conductivity,[11−21,25−27] and decreases in viscosity (see the Supporting Information) with increasing temperature. In accordance with that observation, the D values of **1/2-I$_2$(60)** and **2-I$_2$** gradually increase when the temperature increases from 30 °C to 90 °C (Figure 7a), where the IL exhibits higher diffusion coefficients than the LC electrolyte. On the other hand, the R_s of the **1/2-I$_2$**-DSSC decreases upon heating, while no significant variation is observed for the **2-I$_2$** cell (Figure 7b, top). It should be pointed out that the LC-based solar cell shows higher R_s values at temperatures between 30 °C and 90 °C. Despite this fact, the **1/2-I$_2$**-DSSC shows higher PCE than the **2-I$_2$** cell over 70 °C. These results suggest that other factors than the ability of the electrolytes to transport the ionic components must play a role in the improved LC-DSSCs performances at elevated temperatures.

As for the photovoltaic parameters, a gradual increment in J_{sc}, from 1.06 mA cm^{-2} to 8.72 mA cm^{-2}, when the temperature increases from 30 °C and 90 °C is observed for the DSSC that contains **1/2-I$_2$(60)** (see Figure 6). In contrast, the **2-I$_2$**-based DSSC shows a decrease in J_{sc} value upon heating. These trends in the J_{sc} value can be associated with changes in D, R_s,, and the electron recombination rates at the TiO$_2$/electrolyte interface,[29] where the latter seems to be more pronounced in the IL-based devices. This recombination reaction occurs from the working electrode to the electrolyte and competes with the desired electron injection into the TiO$_2$. When the recombination rate becomes high, the τ value on the TiO$_2$ electrode decays and decreases in V_{oc}, J_{sc}, and PCE are observed.[29] Electrochemical impedance spectroscopy (EIS) (see the Supporting Information) was used to gain information about τ, as a function of temperature for both the LC- and IL-based DSSCs (Figure 7b, bottom). It is of interest that the **1/2-I$_2$(60)**-based cell exhibits longer τ than the IL-based cell. The **1/2-I$_2$(60)** device shows slight τ decay upon heating. However, this tendency is more pronounced for the **2-I$_2$** device (Figure 7b, bottom). These observations show that, at elevated temperatures, the recombination reactions issues become more significant in the IL-based cell than in the LC-based DSSC. Thus, it is evident that a suppression of the recombination loss reaction might occur in the **1/2-I$_2$**-based devices; this effect prevents the decrease in J_{sc} with increasing temperature and is also the reason for the observed high V_{oc}. The high photovoltages obtained are of key importance in the ambitions to identify DSSC systems with very high conversion efficiencies.

It is generally accepted that the V_{oc} value in DSSCs is determined by the difference between the redox potential of the electrolyte and the quasi-Fermi level of the sensitized TiO$_2$ film.[29] The redox potential of the electrolyte is related to the I^-/I_3^- concentration ratio, which is kept constant for all the mixtures, but can also be affected by the solvent or additives. The quasi-Fermi level of TiO$_2$ in DSSCs is usually affected by processes at the semiconductor surface, such as recombination reactions,[50] or interactions with electron-donating species.[51] According to this, we think that a change in the redox potential of the electrolytes and in the quasi-Fermi level of TiO$_2$ electrode induces high V_{oc} values in **1/2-I$_2$**-based DSSCs, which is not observed in the **2-I$_2$** device (see Table 1). In previous works, Grätzel and co-workers also observed increases in the V_{oc} values of DSSCs that contain dyes or electrolyte components bearing hydrophobic groups.[52−54] They attributed this to a suppression of recombination reactions[52] and to the formation of an insulating barrier to the redox carrier in the electrolyte.[53] It seems that these effects are also apparent in the **1/2-I$_2$**-based DSSCs. In the present LC system, the polar carbonate moieties and ionic species (Figure 2) of the **1/2**-based electrolytes probably interact with the TiO$_2$ electrode driving the self-organization along the electrode surface, which spontaneously induces the formation of a nanostructured insulating layer around the TiO$_2$/D35 interface. This spontaneous assembly would act as a barrier against the I_3^- and I^- species, which reduces the local I_3^- concentration at the interface and leads to a decrease in the undesired electron recombination process. This phenomenon would contribute to induce high V_{oc} values in the LC-DSSCs, and combined with the increase in ion diffusion, also enable the enhancement of J_{sc}, FF, and PCE with increasing temperature.

■ CONCLUSION

In summary, a novel type of dye-sensitized solar cell (DSSC) has been developed using two-component liquid-crystalline (LC)-based electrolytes. These LC-DSSCs show significantly high V_{oc} and display an increase in PCE with increasing temperature up to 90 °C. In addition these cells can operate at temperatures up to 120 °C. The reason for these advantagous properties most likely can be traced to the self-organization of the **1/2-I$_2$** electrolyte on the TiO$_2$/D35 surface, which leads to a reduction of the recombination reaction from the working electrode to the electrolyte. These remarkable features qualify LC materials as promising electrolytes for developing DSSCs that can operate efficiently at high temperatures.

■ EXPERIMENTAL SECTION

General. Phase transition behavior was examined by differential scanning calorimetry by using a Netzsch Model DSC 204 Phoenix system. POM observation was conducted with an Olympus Model BX-53 POM system that was equipped with a Linkam Model LTS350 hot stage. Nuclear magnetic resonance (NMR) spectra were recorded at 400 MHz for ^{1}H and 100 MHz for ^{13}C in $CDCl_3$, using a JEOL Model JNM-ECX400 NMR spectrometer. Chemical shifts of H and C NMR signals were quoted to Me_4Si (δ = 0.00) and $CDCl_3$ (δ = 77.00) as internal standards, respectively. FT-IR measurements were conducted with a JASCO Model FT/IR-6100. Matrix-associated laser desorption ionization time-of-flight mass spectra (MALDI-TOF MS) were taken on a Bruker Daltonics Autoflex Speed system, using dithranol as the matrix. Elemental analysis was conducted with a Model CE-440 elemental analyzer (Exeter Analytical, Inc.). X-ray diffractograms were recorded with a Rigaku Model RINT-2500 diffractometer with Ni-filtered Cu Kα radiation and the sample placed in a heating stage. The TiO$_2$ films were printed using a screen printer with a mesh size of 53T. The obtained layer thickness was determined using a Veeco Dektak 150 surface profilometer. The diffusion coefficients of I_3^- were determined by cyclic voltammetry (CV) measured with a HD Hokuto Denko HSV-110 automatic polarization system. The CV was measured using symmetric thin-film cells for **1/2-I$_2$(60)** and microelectrodes for **2-I$_2$** (see the Supporting Information). Viscosity was determined using a Thermo Scientific HAAKE MARS-III rotational rheometer. AM1.5G solar light was simulated with a Yamashita Denso YSS-80 solar simulator. The $I-V$ measurements were conducted with an HD Hokuto Denko HSV-110 automatic polarization system. Electron lifetimes were estimated from EIS experiments measured with a Solartron SI 1287 electrochemical

interface connected to an SI Model 1260 impedance/gain-phase analyzer. The temperature of the cells during the EIS, CV, and linear scanning voltammetry was controlled with a digital hot plate (Dataplate, OMEGA LHS-720 series), and the temperature was verified with an infrared thermometer (A&D Company, Ltd., Model AD-5611A).

Materials. IL **2** was purchased from Aldrich and was used without further purification. All reagents of the highest quality were purchased from Aldrich, Kanto, Tokyo Kasei, or Wako, and were used as received. Unless otherwise noted, all of the reactions were carried out under an argon atmosphere in a dry solvent purchased from Kanto. FTO-coated glass substrates (Pilkington, TEC15) were purchased from Hartford Glass Co. The D35 sensitizer was obtained from Dyenamo AB. TiO_2 paste (Dyesol, NR-T90) and Surlyn hot melt plastic were purchased from Dyesol, Ltd.

Preparation of 1/2 Mixtures. Electrolytes **1**/**2** were obtained by mixing **2**-$\mathbf{I_2}$ and compound **1** in different ratios. **2**-$\mathbf{I_2}$ was prepared by the addition of 20 mol % of I_2 to a previously weighed amount of compound **2**. This mixture was diluted in a known volume of acetonitrile (ACN). The appropriate volume of the **2**-$\mathbf{I_2}$ solution was added to compound **1** in a dry microtube using a micropipette. The mixture was completely solubilized by adding the required volume of ACN and then the solvent was removed by rotary evaporation. The samples were dried under vacuum at 40 °C for 12 h prior to their use in the solar cell devices.

Fabrication of DSSCs. *Working Electrodes.* The working electrodes were fabricated as follows. FTO-coated glass substrates (1.7 cm × 1.7 cm) were immersed in a 40 mM $TiCl_4$ water solution at 70 °C for 90 min. The substrates were then rinsed with water and ethanol. One layer (0.5 cm × 0.5 cm) of Dyesol 90 NR-T paste was screen-printed on the FTO substrates. The electrodes were sintered at 500 °C for 30 min and then immersed in a 40 mM $TiCl_4$ water solution, which was kept at 70 °C for 30 min. The electrodes were sintered again at 500 °C for 30 min and cooled to 80 °C. The hot electrodes were directly immersed in a 0.2 mM ethanol solution of the D35 dye sensitizer[48] for 24 h. The electrodes were then rinsed with ethanol and dried under ambient conditions before their use.

Counter-electrodes. The counter-electrodes were fabricated as follows. A 5 mM solution of H_2PtCl_6 in ethanol was dropcast (10 μL per cm^2) onto FTO substrates (1.7 cm × 1.7 cm). The substrates were then sintered at 390 °C for 30 min.[55]

Dye-Sensitized Solar Cells (DSSCs). The DSSCs were assembled as follows. The appropriate amount of the electrolyte mixture (~5 mg) was carefully placed on the TiO_2 electrode with a spatula for the **1**/**2**-$\mathbf{I_2}$ mixtures and with a micropipette for **2**-$\mathbf{I_2}$. A 30-μm-thick Surlyn hot melt plastic with a frame size of 7 mm × 7 mm was placed around the electrolyte coated TiO_2 electrode. This electrode was then covered with the platinized counter-electrode and pressed together with two clips. The cells were sealed by heating at 120 °C for 3 min (the melting point of Surlyn plastic is 93 °C) and then cooled at rt prior to the photovoltaic studies. In the case of the experiments that were conducted at temperatures of >90 °C, the cells were sealed by heating at 155 °C for 3 min, using Bynel hot melt plastic (50 μm thick) as a sealant. The active area of each cell is 0.25 cm^2.

■ ASSOCIATED CONTENT

Ⓢ Supporting Information

Synthesis and characterization of compound **1**. LC properties of **1** and **1**/**2**-$\mathbf{I_2}$ mixtures including DSC traces, XRD studies, and POM images of **1** and **1**/**2**-$\mathbf{I_2}$ mixtures. Viscosity of **1**/**2**-$\mathbf{I_2}$ and **2**-$\mathbf{I_2}$ as a function of temperature. SEM image and height profile of the TiO_2 electrode. Molecular structure of the D35 sensitizer. *I*−*V* curves of the **1**/**2**-$\mathbf{I_2}$- and **2**-$\mathbf{I_2}$-based DSSCs. Photovoltaic parameters of **1**/**2**-$\mathbf{I_2}$- and **2**-$\mathbf{I_2}$-based DSSCs as a function of temperature. R_s of the **1**/**2**-$\mathbf{I_2}$- and **2**-$\mathbf{I_2}$-based DSSCs, as a function of temperature. CV and EIS experiments. This material is available free of charge via the Internet at http://pubs.acs.org.

■ AUTHOR INFORMATION

Corresponding Author

*E-mail: kato@chiral.t.u-tokyo.ac.jp.

Notes

The authors declare no competing financial interest.

■ ACKNOWLEDGMENTS

This study was partially supported by the Funding Program for World-Leading Innovative R&D on Science and Technology (FIRST) from the Cabinet Office, Government of Japan. This work was also partially supported by a Grant-in-Aid for Scientific Research (No. 22107003) in the Innovative Area of "Fusion Materials" (Area No. 2206) from the Ministry of Education, Culture, Sports, Science and Technology (MEXT). D.H. is grateful for financial support from the Sweden−Japan Foundation.

■ REFERENCES

(1) Goodby, J. W.; Collings, P. J.; Kato, T.; Tschierske, C.; Gleeson, H.; Raynes, P. *Handbook of Liquid Crystals*, 2nd Edition; Wiley−VCH: Weinheim, Germany, 2014.

(2) Kato, T. *Angew. Chem., Int. Ed.* **2010**, *49*, 7847.

(3) Kato, T. *Science* **2002**, *295*, 1414.

(4) Gin, D. L.; Lu, X. Y.; Nemade, P. R.; Pecinovsky, C. S.; Xu, Y. J.; Zhou, M. J. *Adv. Funct. Mater.* **2006**, *16*, 865.

(5) Wiesner, U.; Cho, B.-K.; Jain, A.; Gruner, S. M. *Science* **2004**, *305*, 1598.

(6) Tschierske, C. *Angew. Chem., Int. Ed.* **2013**, *52*, 8828.

(7) Wu, J.; Pisula, W.; Müllen, K. *Chem. Rev.* **2007**, *107*, 718.

(8) Sergeyev, S.; Pisula, W.; Geerts, Y. H. *Chem. Soc. Rev.* **2007**, *36*, 1902.

(9) Chen, S.; Eichhorn, S. H. *Isr. J. Chem.* **2012**, *52*, 830.

(10) Broer, D. J.; Bastiaansen, C. M. W.; Debije, M. G.; Schenning, A. P. H. J. *Angew. Chem., Int. Ed.* **2012**, *51*, 7102.

(11) Yoshio, M.; Mukai, T.; Ohno, H.; Kato, T. *J. Am. Chem. Soc.* **2004**, *126*, 994.

(12) Yoshio, M.; Kagata, T.; Hoshino, K.; Mukai, T.; Ohno, H.; Kato, T. *J. Am. Chem. Soc.* **2006**, *128*, 5570.

(13) Yoshio, M.; Mukai, T.; Kanie, K.; Yoshizawa, M.; Ohno, H.; Kato, T. *Adv. Mater.* **2002**, *14*, 351.

(14) Ichikawa, T.; Yoshio, M.; Hamasaki, A.; Taguchi, S.; Liu, F.; Zeng, X. B.; Ungar, G.; Ohno, H.; Kato, T. *J. Am. Chem. Soc.* **2012**, *134*, 2634.

(15) Kerr, R. L.; Miller, S. A.; Shoemaker, R. K.; Elliot, B. J.; Gin, D. L. *J. Am. Chem. Soc.* **2009**, *131*, 15972.

(16) Ichikawa, T.; Yoshio, M.; Hamasaki, A.; Mukai, T.; Ohno, H.; Kato, T. *J. Am. Chem. Soc.* **2007**, *129*, 10662.

(17) Binnemans, K. *Chem. Rev.* **2005**, *105*, 4148.

(18) Kato, T.; Mizoshita, N.; Kishimoto, K. *Angew. Chem., Int. Ed.* **2006**, *45*, 38.

(19) Yoshio, M.; Kato, T. In *Handbook of Liquid Crystals*, 2nd Edition; Goodby, J. W., Collings, P. J., Kato, T., Tschierske, C., Gleeson, H., Raynes, P., Eds.; Wiley−VCH: Weinheim, Germany, 2014; Vol. *8*, Chapter 23, p 727.

(20) Lowe, A. M.; Abbott, N. L. *Chem. Mater.* **2011**, *24*, 746.

(21) Soberats, B.; Yoshio, M.; Ichikawa, T.; Taguchi, S.; Ohno, H.; Kato, T. *J. Am. Chem. Soc.* **2013**, *135*, 15286.

(22) Yamanaka, N.; Kawano, R.; Kubo, W.; Kitamura, T.; Wada, Y.; Watanabe, M.; Yanagida, S. *Chem. Commun.* **2005**, 740.

(23) Yamanaka, N.; Kawano, R.; Kubo, W.; Masaki, N.; Kitamura, T.; Wada, Y.; Watanabe, M.; Yanagida, S. *J. Phys. Chem. B* **2007**, *111*, 4763.

(24) Costa, R. D.; Werner, F.; Wang, X. J.; Gronninger, P.; Feihl, S. F.; Kohler, T. U.; Wasserscheid, P.; Hibler, S.; Beranek, R.; Meyer, K.; Guldi, D. M. *Adv. Energy Mater.* **2013**, *3*, 657.

(25) Shimura, H.; Yoshio, M.; Hoshino, K.; Mukai, T.; Ohno, H.; Kato, T. *J. Am. Chem. Soc.* **2008**, *130*, 1759.

(26) Ichikawa, T.; Yoshio, M.; Taguchi, S.; Kagimoto, J.; Ohno, H.; Kato, T. *Chem. Sci.* **2012**, *3*, 2001.
(27) Yoshio, M.; Mukai, T.; Yoshizawa, M.; Ohno, H.; Kato, T. *Mol. Cryst. Liq. Cryst.* **2004**, *413*, 99.
(28) O'Regan, B.; Grätzel, M. *Nature* **1991**, *353*, 737.
(29) Hagfeldt, A.; Boschloo, G.; Sun, L.; Kloo, L.; Pettersson, H. *Chem. Rev.* **2010**, *110*, 6595.
(30) Hinsch, A.; Kroon, J. M.; Kern, R.; Uhlendorf, I.; Holzbock, J.; Meyer, A.; Ferber, J. *Prog. Photovoltaics* **2001**, *9*, 425.
(31) Uchida, S.; Inoue, T.; Kubo, T.; Segawa, H. In *Trends in Advanced Sensitized and Organic Solar Cells*; Miyasaka, T., Ed.; CMC Publishing: Tokyo, 2012; p 144.
(32) Uchida, S.; Inoue, T.; Kubo, T.; Segawa, H. *Mater. Res. Soc. Symp. Proc.* **2010**, *1211*, R09.
(33) Bai, Y.; Cao, Y.; Zhang, J.; Wang, M.; Li, R.; Wang, P.; Zakeeruddin, S. M.; Grätzel, M. *Nat. Mater.* **2008**, *7*, 626.
(34) Gorlov, M.; Kloo, L. *Dalton Trans.* **2008**, 2655.
(35) de Freitas, J. N.; Nogueira, A. F.; De Paoli, M.-A. *J. Mater. Chem.* **2009**, *19*, 5279.
(36) Wang, P.; Zakeeruddin, S. M.; Moser, J. E.; Nazeeruddin, M. K.; Sekiguchi, T.; Grätzel, M. *Nat. Mater.* **2003**, *2*, 402.
(37) Yanagida, S.; Watanabe, M.; Matsui, H.; Okada, K.; Usui, H.; Ezure, T.; Tanabe, N. *Fujikura Technol. Rev.* **2005**, *34*, 59.
(38) Chung, I.; Lee, B.; He, J. Q.; Chang, R. P. H.; Kanatzidis, M. G. *Nature* **2012**, *485*, 486.
(39) Sebastián, P. J.; Olea, A.; Campos, J.; Toledo, J. A.; Gamboa, S. A. *Sol. Energy Mater. Sol. Cells* **2004**, *81*, 349.
(40) Grätzel, M. *Prog. Photovoltaics* **2006**, *14*, 429.
(41) Raga, S. R.; Fabregat-Santiago, F. *Phys. Chem. Chem. Phys.* **2013**, *15*, 2328.
(42) Paulsson, H.; Hagfeldt, A.; Kloo, L. *J. Phys. Chem. B* **2003**, *107*, 13665.
(43) Marszalek, M.; Arendse, F. D.; Decoppet, J.-D.; Babkair, S. S.; Ansari, A. A.; Habib, S. S.; Wang, M.; Zakeeruddin, S. M.; Grätzel, M. *Adv. Energy Mater.* **2014**, *4*, 1301235.
(44) Berginc, M.; Krasovec, U. O.; Hocevar, M.; Topic, M. *Thin Solid Films* **2008**, *516*, 7155.
(45) Berginc, M.; Krasovec, U. O.; Jankovec, M.; Topic, M. *Sol. Energy Mater. Sol. Cells* **2007**, *91*, 821.
(46) Wachter, P.; Zistler, M.; Schreiner, C.; Berginc, M.; Krasovec, U. O.; Gerhard, D.; Wasserscheid, P.; Hinsch, A.; Gores, H. J. *J. Photochem. Photobiol., A* **2008**, *197*, 25.
(47) Jiang, X.; Karlsson, K. M.; Gabrielsson, E.; Johansson, E. M. J.; Quintana, M.; Karlsson, M.; Sun, L.; Boschloo, G.; Hagfeldt, A. *Adv. Funct. Mater.* **2011**, *21*, 2944.
(48) Feldt, S. M.; Gibson, E. A.; Gabrielsson, E.; Sun, L.; Boschloo, G.; Hagfeldt, A. *J. Am. Chem. Soc.* **2010**, *132*, 16714.
(49) Total electrical resistances were calculated by using Ohm's Law ($I = V/R$) at the slope of the $I-V$ curves, near V_{oc}.
(50) Berginc, M.; Krasovec, U. O.; Topic, M. *Phys. Status Solidi A* **2013**, *210*, 1750.
(51) Katoh, R.; Kasuya, M.; Kodate, S.; Furube, A.; Fuke, N.; Koide, N. *J. Phys. Chem. C* **2009**, *113*, 20738.
(52) Kawano, R.; Nazeeruddin, M. K.; Sato, A.; Grätzel, M.; Watanabe, M. *Electrochem. Commun.* **2007**, *9*, 1134.
(53) Koh, T. M.; Li, H.; Nonomura, K.; Mathews, N.; Hagfeldt, A.; Grätzel, M.; Mhaisalkar, S. G.; Grimsdale, A. C. *Chem. Commun.* **2013**, *49*, 9101.
(54) Wang, P.; Zakeeruddin, S. M.; Comte, P.; Charvet, R.; Humphry-Baker, R.; Grätzel, M. *J. Phys. Chem. B* **2003**, *107*, 14336.
(55) Papageorgiou, N.; Maier, W. F.; Grätzel, M. *J. Electrochem. Soc.* **1997**, *144*, 876.